Progress In Electromagnetics Research B, Vol. 70, 13–26, 2016

Hierarchical Layer-Multiple-Scattering Theory for Metamaterials of Clusters of Nonspherical Particles

Vassilios Yannopapas*

Abstract—We present a hierarchical layer-multiple-scattering method of electromagnetic waves for the study of photonic structures consisting of many-scatterers per unit cell (clusters of scatterers) where the scatterers are in general non-spherical and/or anisotropic or inhomogeneous. Our approach is a two-stage process where we take into account all the multiple-scattering events involved: (a) among the scatterers of the cluster comprising the unit cell of the structure, and (b) among the clusters within the structure. As text cases, we model the optical properties of plasmonic metamaterials made from clusters of gold nanocubes.

1. INTRODUCTION

Artificial photonic structures fall within three main categories: photonic crystals, plasmonic crystals and metamaterials. Photonic crystals possess an absolute band gap, i.e., a frequency region where no electromagnetic (EM) Bloch modes are allowed as a result of destructive interference allowing for the passive control of light emission and flow within their volume. Plasmonic materials and metamaterials operate both in the subwavelength regime, i.e., around the center of the Brillouin zone. Plasmonic materials are mainly used for boosting electric field in small volumes and tailoring light absorption. Metamaterials have more unconventional features such as negative refractive index and/or magnetic permeability with application in optical microscopy, imaging and cloaking.

An indispensable theoretical tool for the modelling of photonic structures is the multiple-scattering method for electromagnetic (EM) waves. There are two basic variations of the multiple-scattering method: the bulk and the layer-multiple-scattering one. In the bulk multiple-scattering theory, one deals with an infinitely periodic crystal and obtains the energy band structure for electrons in atomic solids [1], or the frequency band structure for classical (EM and elastic) waves [2, 3]. In the layer-multiple-scattering (LMS) formulation, one assumes periodic arrangement of scatterers in two dimensions (2D) offering the possibility for the study of various configurations such as a single plane (monolayer) of scatterers, a finite slab of several planes or scatterers or an infinitely periodic three-dimensional (3D) crystal viewed as a succession of planes parallel to a given crystallographic direction. Within a given 2D lattice (plane) of spheres, the EM field is written in terms of vector spherical waves and is obtained via the multiple-scattering technique. In the space between two consecutive planes, the EM field is written in a plane wave basis where the multiple-scattering between the planes is taken into account fully. A slab of macroscopic thickness, i.e., containing several hundreds of planes of spheres, can be easily built up via a doubling-layer process [4–6]. By imposing boundary conditions along the growth direction of the crystal slab, one can also calculate the complex frequency band structure [4–6].

The LMS method has been mainly applied to model the optical properties of colloidal photonic crystals and metamaterials of spherical scatterers which are usually realized by self-assembly. After being generalized to treat non-spherical axi-symmetric scatterers [7, 8], the LMS method can simulate

Received 21 July 2016, Accepted 13 September 2016, Scheduled 26 September 2016
* Corresponding author: Vassilios Yannopapas (vyannop@mail.ntua.gr).
The author is with the Department of Physics, National Technical University of Athens, Athens GR-157 80, Greece.

lithography-based structures such as arrays of plasmonic nanodisks and nanorods [9, 10]. Recently, the LMS has been extended so as to treat anisotropic spherical scatterers [11, 12] whereby non-reciprocal structures such as arrays of magnetized plasma spheres [13]. In order to model metamaterials consisting of clusters of metallic nanoparticles [14, 15], the LMS has been generalized so that it can accommodate many spheres per unit cell [16]. Lastly, a hybrid discrete-dipole approximation (DDA)/LMS method has been developed so that the LMS can treat photonic structures of general scatterers, i.e., scatterers of general (non-spherical) shape which might be anisotropic and/or inhomogeneous [17]. In this work, we aim at merging the many-spheres per unit cell formalism of [16] with that of the hybrid DDA/LMS method of [17] so that it can tackle photonic structures with many scatterers per unit cell where the scatterers can in general be non-spherical, anisotropic and/or inhomogeneous. Such structures are known as hierarchical metamaterials, and their modelling with standard EM solvers is very challenging due to the involvement of two different length scales, i.e., the characteristic interparticle distance within the cluster and the lattice constant (period) of the metamaterial. The latter, however, constitutes the principle advantage of the presented method, i.e., the ability to deal with two different length scales so as to simulate the optical response of hierarchical metamaterials. In the following, we present the mathematical formalism of the developed many-scatterer per unit cell hybrid DDA/LMS method as well as an application to the case of plasmonic structures made from clusters of gold nanocubes.

2. MULTIPOLE EXPANSION OF THE EM FIELD

Let us consider a harmonic EM wave of angular frequency ω which is described by its electric-field component

$$\mathbf{E}(\mathbf{r},t) = \mathrm{Re}\left[\mathbf{E}(\mathbf{r})\exp(-\mathrm{i}\omega t)\right]. \tag{1}$$

In a homogeneous medium characterized by a dielectric function $\epsilon(\omega)\epsilon_0$ and a magnetic permeability $\mu(\omega)\mu_0$, where ϵ_0, μ_0 are the electric permittivity and magnetic permeability of vacuum, Maxwell equations imply that $\mathbf{E}(\mathbf{r})$ satisfies a vector Helmholtz equation, subject to the condition $\nabla\cdot\mathbf{E}=0$, with a wave number $q=\omega/c$, where $c=1/\sqrt{\mu\epsilon\mu_0\epsilon_0}=c_0/\sqrt{\mu\epsilon}$ is the velocity of light in the medium. The spherical-wave expansion of $\mathbf{E}(\mathbf{r})$ is given by [18]

$$\mathbf{E}(\mathbf{r}) = \sum_{l=1}^{\infty}\sum_{m=-l}^{l}\left\{a_{lm}^{H} f_l(qr)\mathbf{X}_{lm}(\hat{\mathbf{r}}) + a_{lm}^{E}\frac{\mathrm{i}}{q}\nabla\times\left[f_l(qr)\mathbf{X}_{lm}(\hat{\mathbf{r}})\right]\right\}, \tag{2}$$

where a_{lm}^{P} $(P=E,H)$ are coefficients to be determined. $\mathbf{X}_{lm}(\hat{\mathbf{r}})$ are the so-called vector spherical harmonics [18], and f_l may be any linear combination of the spherical Bessel function, j_l, and the spherical Hankel function, h_l^+. The corresponding magnetic induction, $\mathbf{B}(\mathbf{r})$, can be readily obtained from $\mathbf{E}(\mathbf{r},t)$ using Maxwell's equations,

$$\mathbf{B}(\mathbf{r}) = \frac{\sqrt{\epsilon\mu}}{c_0}\sum_{l=1}^{\infty}\sum_{m=-l}^{l}\left\{a_{lm}^{E} f_l(qr)\mathbf{X}_{lm}(\hat{\mathbf{r}}) - a_{lm}^{H}\frac{\mathrm{i}}{q}\nabla\times\left[f_l(qr)\mathbf{X}_{lm}(\hat{\mathbf{r}})\right]\right\}, \tag{3}$$

and we shall not write it down explicitly in what follows.

3. SCATTERING BY A SINGLE SPHERICAL SCATTERER

In this section, we present a brief summary of the solution to the problem of EM scattering from a single sphere (Mie scattering theory [18, 19]). We will make use of the compact notation of [20] for the eigenfunctions and the angular-momentum indices, which allows for easier computer coding.

We consider a sphere of radius S, with its center at the origin of coordinates, and assume that its electric permittivity ϵ_s and/or magnetic permeability μ_s are different from those, ϵ_h, μ_h, of the surrounding homogeneous medium. An EM plane wave incident on this scatterer is described, respectively, by Eq. (2) with $f_l = j_l$ (since the plane wave is finite everywhere) and appropriate coefficients a_L^0, where L denotes collectively the indices Plm. That is,

$$\mathbf{E}^0(\mathbf{r}) = \sum_L a_L^0\mathbf{J}_L(\mathbf{r}) \tag{4}$$

where

$$\mathbf{J}_{Elm}(\mathbf{r}) = \frac{\mathrm{i}}{q_h}\nabla \times j_l(q_h r)\mathbf{X}_{lm}(\hat{\mathbf{r}}), \quad \mathbf{J}_{Hlm}(\mathbf{r}) = j_l(q_h r)\mathbf{X}_{lm}(\hat{\mathbf{r}}) \tag{5}$$

and $q_h = \sqrt{\epsilon_h \mu_h}\omega/c_0$. The coefficients a_L^0 depend on the amplitude, polarization and propagation direction of the incident EM plane wave [4–6, 18].

Similarly, the wave that is scattered from the sphere is described by Eq. (2) with $f_l = h_l^+$, which has the asymptotic form appropriate to an outgoing spherical wave: $h_l^+ \approx (-\mathrm{i})^l \exp(\mathrm{i}q_h r)/\mathrm{i}q_h r$ as $r \to \infty$, and appropriate expansion coefficients a_L^+. Namely,

$$\mathbf{E}^+(\mathbf{r}) = \sum_L a_L^+ \mathbf{H}_L(\mathbf{r}) \tag{6}$$

where

$$\mathbf{H}_{Elm}(\mathbf{r}) = \frac{\mathrm{i}}{q_h}\nabla \times h_l^+(q_h r)\mathbf{X}_{lm}(\hat{\mathbf{r}}), \quad \mathbf{H}_{Hlm}(\mathbf{r}) = h_l^+(q_h r)\mathbf{X}_{lm}(\hat{\mathbf{r}}). \tag{7}$$

The wavefield for $r > S$ is the sum of the incident and scattered waves, i.e., $\mathbf{E}^{out} = \mathbf{E}^0 + \mathbf{E}^+$. The spherical-wave expansion of the field $\mathbf{E}^I$ for $r < R$ (inside the sphere) is obtained in a similar manner by the requirement that it is finite at the origin ($\mathbf{r} = \mathbf{0}$), i.e.,

$$\mathbf{E}^I(\mathbf{r}) = \sum_L a_L^I \mathbf{J}_L^s(\mathbf{r}) \tag{8}$$

where $\mathbf{J}_L^s(\mathbf{r})$ are given from Eq. (5) by replacing q_h with $q_s = \sqrt{\epsilon_s \mu_s}\omega/c_0$.

By applying the requirement that the tangential components of $\mathbf{E}$ and $\mathbf{H}$ are continuous at the surface of the scatterer, we obtain a relation between the expansion coefficients of the incident and the scattered field, as follows:

$$a_L^+ = \sum_{L'} T_{LL'} a_{L'}^0, \tag{9}$$

where $T_{LL'}$ are the elements of the so-called scattering transition T-matrix [19]. Eq. (9) is valid for any shape of scatterer; for spherically symmetric scatterers, each spherical wave scatters independently of all others, which leads to a transition T-matrix which does not depend on m and is diagonal in l, i.e., $T_{LL'} = T_L \delta_{LL'}$; it is given by

$$T_{El}(\omega) = \left[\frac{j_l(q_s r)\frac{\partial}{\partial r}\left(r j_l(q_h r)\right)\epsilon_s - j_l(q_h r)\frac{\partial}{\partial r}\left(r j_l(q_s r)\right)\epsilon_h}{h_l^+(q_h r)\frac{\partial}{\partial r}\left(r j_l(q_s r)\right)\epsilon_h - j_l(q_s r)\frac{\partial}{\partial r}\left(r h_l^+(q_h r)\right)\epsilon_s} \right]_{r=S} \tag{10}$$

$$T_{Hl}(\omega) = \left[\frac{j_l(q_s r)\frac{\partial}{\partial r}\left(r j_l(q_h r)\right)\mu_s - j_l(q_h r)\frac{\partial}{\partial r}\left(r j_l(q_s r)\right)\mu_h}{h_l^+(q_h r)\frac{\partial}{\partial r}\left(r j_l(q_s r)\right)\mu_h - j_l(q_s r)\frac{\partial}{\partial r}\left(r h_l^+(q_h r)\right)\mu_s} \right]_{r=S} \tag{11}$$

4. MULTIPLE-SCATTERING BY A NON-SPHERICAL SCATTERER

4.1. Discrete Dipole Approximation

Next, we study the optical response of a generally anisotropic scatterer of arbitrary shape using the DDA [21–23]. The scattering object is considered as an array of point dipoles ($i = 1, \ldots, N$), each of which is located at the position $\mathbf{r}_i$ and corresponds to a dipole moment $\mathbf{P}_i$ and a (position-dependent) polarizability tensor $\tilde{\alpha}_i$. The above quantities are connected by

$$\mathbf{P}_i = \tilde{\alpha}_i \mathbf{E}_i \tag{12}$$

where $\mathbf{E}_i$ is the electric field at i-th dipole,

$$\mathbf{E}_i = \mathbf{E}_i^0 - \sum_{j \neq i} \mathbf{A}_{ij} \cdot \mathbf{P}_j \tag{13}$$

which consists of the directly incident field $\mathbf{E}_i^0$ as well as the field scattered by all the other dipoles $j \neq i$, and it is incident on the i-th dipole [second term of Eq. (13)]. The interaction matrix $\mathbf{A}_{ij}$ is given from

$$\mathbf{A}_{ij} = \frac{\exp(ikr_{ij})}{r_{ij}} \left[k^2 \left(\hat{r}_{ij}\hat{r}_{ij} - \mathbf{1}_3 \right) + \frac{ikr_{ij} - 1}{r_{ij}^2} \left(3\hat{r}_{ij}\hat{r}_{ij} - \mathbf{1}_3 \right) \right], \quad i \neq j \tag{14}$$

where $\mathbf{1}_3$ is the 3×3 unit matrix, $\mathbf{r}_{ij} = \mathbf{r}_i - \mathbf{r}_j$, $\hat{\mathbf{r}}_{ij} = \mathbf{r}_{ij}/|\mathbf{r}_{ij}|$. By combining Eqs. (12) to (14) we obtain a linear system of equations, i.e.,

$$\sum_{j=1}^{N} \mathbf{A}_{ij}\mathbf{P}_j = \mathbf{E}_i^0 \tag{15}$$

where the diagonal elements of the interaction matrix are essentially the inverse of the polarizability tensor of each dipole, i.e.,

$$\mathbf{A}_{ii} = [\tilde{\alpha}_i]^{-1}. \tag{16}$$

For an anisotropic sphere characterized by a dielectric tensor $\tilde{\epsilon}_s$ and immersed within an isotropic host of dielectric constant ϵ_h, the polarizability tensor of the sphere is given by the Clausius-Mossoti formula for anisotropic spheres, that is

$$\tilde{\alpha}_i = V_s \frac{3\epsilon_h}{4\pi} \left[\tilde{\epsilon}_s - \epsilon_h \mathbf{1}_3 \right] \left[\tilde{\epsilon}_s + 2\epsilon_h \mathbf{1}_3 \right]^{-1}. \tag{17}$$

Equation (15) is preferentially solved by conjugate-gradient-type solvers for fast convergence [24]. Having determined the dipole moment $\mathbf{P}_i$ at each point dipole, one can calculate quantities such as the scattering, extinction and absorption cross sections [21–23].

The scattered field $\mathbf{E}^+(\mathbf{r}_p)$ at a given point $\mathbf{r}_p$ in space is the sum of the (secondary) field emitted by each dipole into which the actual scatterer is discretized, i.e.,

$$\mathbf{E}^+(\mathbf{r}_p) = \sum_i \mathbf{A}_{pi}\mathbf{P}_i \tag{18}$$

where $\mathbf{A}_{pi}$ is provided by Eq. (14), and the point in space does not coincide with one of the dipoles ($\mathbf{r}_p \neq \mathbf{r}_i$). The polarization vectors $\mathbf{P}_i$ at each point dipole are provided by Eq. (15).

4.2. Calculation of the *T*-Matrix via Point-Matching

The point-matching (PM) method for calculating the T-matrix of general scatterers has been first proposed in [25]. Here, we restate the DDA-based PM method in the spirit of the LMS formalism [16]. Note in passing that a PM method for the calculation of the T-matrix has also been presented in conjunction with the FDTD method [26]. Moreover, the PM method has been employed for obtaining the T-matrix and the multipole moments for a collection of spherical scatterers [27].

We assume that a single spherical EM wave is incident on an arbitrary scatterer, i.e., $\mathbf{E}^0(\mathbf{r}) = \mathbf{J}_{L_0}(\mathbf{r})$. This means that in Eq. (9) we set $a_L^0 = \delta_{LL_0}$ which becomes

$$a_L^+ = T_{LL_0}. \tag{19}$$

Equation (6) becomes

$$\sum_L T_{LL_0}\mathbf{H}_L(\mathbf{r}_p) = \mathbf{E}^+(\mathbf{r}_p) \tag{20}$$

The matrix elements of the L_0-column of the T-matrix can be calculated from the above equation provided that we know the scattered field $\mathbf{E}^+$ at a sufficient number of points $\mathbf{r}_p$ in space. Eq. (20) must be solved for different incident spherical waves $\mathbf{J}_{L_0}$ in order to obtain all the T-matrix columns. Namely, we calculate the scattered field via DDA [Eq. (18)] at several points on a spherical surface surrounding the scatterer so that Eq. (20) becomes a linear system of equations for the T-matrix elements. However, in practice, we calculate the scattered field $\mathbf{E}^+$ via DDA at a large number of points so that the unknowns T_{LL_0} are fewer than the system equations. In this case, Eq. (20) is solved by seeking a least-squares solution.

The scattering/extinction and absorption cross sections of light scattered off a single scatterer can be calculated in a spherical wave expansion by use of the obtained T-matrix — see Eq. (15) of [7].

5. MULTIPLE SCATTERING BY MANY SCATTERERS

5.1. Multiple Scattering by a Cluster of Scatterers

Next we consider a collection of N_s nonoverlapping spherical scatterers centered at sites $\mathbf{R}_n$ in a homogeneous host medium. An outgoing vector spherical wave about $\mathbf{R}_{n'}$ can be expanded in a series of incoming vector spherical waves around $\mathbf{R}_n$ as follows

$$\mathbf{H}_{L'}\left(\mathbf{r}-\mathbf{R}_{n'}\right)=\sum_{L}\Omega_{LL'}^{nn'}\mathbf{J}_{L}\left(\mathbf{r}-\mathbf{R}_{n}\right). \tag{21}$$

An outgoing vector spherical wave about $\mathbf{R}_{n'}$ can be expanded in a series of outgoing vector spherical waves around $\mathbf{R}_n$ as follows

$$\mathbf{H}_{L'}\left(\mathbf{r}-\mathbf{R}_{n'}\right)=\sum_{L}\Xi_{LL'}^{nn'}\mathbf{H}_{L}\left(\mathbf{r}-\mathbf{R}_{n}\right). \tag{22}$$

and similarly for incoming vector spherical waves

$$\mathbf{J}_{L'}\left(\mathbf{r}-\mathbf{R}_{n'}\right)=\sum_{L}\Xi_{LL'}^{nn'}\mathbf{J}_{L}\left(\mathbf{r}-\mathbf{R}_{n}\right). \tag{23}$$

Explicit formulae for the matrices $\mathbf{\Omega}$ and Ξ are given elsewhere [16]. These matrices do not depend on the material properties of the scatterers but on their particular arrangement in space. From Eq. (21) we can express an outgoing EM wave about $\mathbf{R}_{n'}$, $\sum_{L'} b_{L'}^{+n'}\mathbf{H}_{L'}(\mathbf{r}-\mathbf{R}_{n'})$, as an incoming EM wave about $\mathbf{R}_n$, $\sum_L b_L^{'n}\mathbf{J}_L(\mathbf{r}-\mathbf{R}_n)$, as follows

$$b_{L}^{'n}(n')=\sum_{L'}\Omega_{LL'}^{nn'}b_{L'}^{+n'}. \tag{24}$$

The wave scattered from the sphere at $\mathbf{R}_n$ is determined by the total incident wave on that sphere, i.e.,

$$b_{L}^{+n}=\sum_{L'}T_{LL'}^{n}\left[a_{L'}^{0n}+\sum_{n'\neq n}b_{L'}^{'n}(n')\right], \tag{25}$$

where $T_{LL'}^{n}=T_{L}^{n}\delta_{LL'}$ is the T-matrix for the sphere at $\mathbf{R}_n$, and a_L^{0n} are the spherical-wave expansion coefficients of an externally incident wave. Eq. (25) can be written as

$$\sum_{n'L'}\left[\delta_{nn'}\delta_{LL'}-\sum_{L''}T_{LL''}^{n}\Omega_{L''L'}^{nn'}\right]b_{L'}^{+n'}=\sum_{L'}T_{LL'}^{n}a_{L'}^{0n}. \tag{26}$$

The above equation is the basic equation of multiple scattering and can be solved either by standard linear-system numerical solvers or iteratively [28]. The solution provides the scattering wave b_L^{+n} outgoing from each sphere of the collection for a given externally incident wave a_L^{0n}. Having calculated b_L^{+n} from Eq. (26) one can readily find the coefficients $b_L^{'n}(n')$ from Eq. (24) and therefore the total incident wave to each sphere of the collection given by the square brackets of Eq. (25).

The electric field outside the spheres, $\mathbf{E}^{out}$, is written as the sum of the scattered field from all spheres plus the incident wave field, i.e.,

$$\mathbf{E}^{out}(\mathbf{r})=\mathbf{E}^{sc}(\mathbf{r})+\mathbf{E}^{0}(\mathbf{r}) \tag{27}$$

where the incident field $\mathbf{E}^0$ is given by Eq. (4), and $\mathbf{E}^{sc}$ is given as follows

$$\mathbf{E}^{sc}(\mathbf{r})=\sum_{n=1}^{N_s}\sum_{L}b_{L}^{+n}\mathbf{H}_{L}\left(\mathbf{r}-\mathbf{R}_{n}\right). \tag{28}$$

In order to incorporate of a cluster of spherical scatterers within the existing LMS code as single scattering entity, we need to calculate the scattering T-matrix $T_{LL'}^{cl}$ of the entire cluster. It can be shown that the scattering matrix $T_{LL'}^{cl}$ assumes the form [20]

$$T_{LL'}^{cl}=\sum_{nn'}\sum_{L''L'''}\Xi_{LL''}^{0n}\left[\left[\mathbf{I}-\mathbf{T}\mathbf{\Omega}\right]^{-1}\mathbf{T}\right]_{L''L'''}^{nn'}\Xi_{L'''L'}^{n'0}, \tag{29}$$

where the matrix $[\mathbf{I} - \mathbf{T\Omega}]$ is the one appearing in the left-hand side of Eq. (26). $T^{cl}_{LL'}$ contains nondiagonal elements in general. We note that alternative formulations of the EM scattering by a finite number of scatterers were developed in the past [2, 3]. However, the formalism presented above is suitable for embedding the T-matrix of Eq. (29) in the existing LMS formalism.

5.2. Multiple-Scattering within a 2D Plane of Scatterers

The structures that we are interested in usually contain more than one plane of scatterers, but to begin with, we consider just one plane, at $z = 0$, in which case the single scatterers or the clusters of scatterers, which do not overlap with each other, are centred on the sites $\mathbf{R}_n$ of a given 2D lattice. We define the 2D reciprocal vectors $\mathbf{g}$ and the surface Brillouin zone (SBZ) corresponding to this lattice in the usual manner [5, 6].

Let the plane wave, described by Eq. (1), be incident on this plane of (single or clusters of) scatterers. We can always write the component of its wavevector parallel to the plane of scatterers, as follows

$$\mathbf{q}_{\parallel} = \mathbf{k}_{\parallel} + \mathbf{g}' \tag{30}$$

where the reduced wavevector $\mathbf{k}_{\parallel}$ lies in the SBZ, and $\mathbf{g}'$ is a certain reciprocal vector. In what follows, we shall write the wavevector of a plane wave of given $q = \sqrt{\mu\epsilon}\omega/c$ and given $\mathbf{q}_{\parallel} = \mathbf{k}_{\parallel} + \mathbf{g}$ as follows

$$\mathbf{K}^{\pm}_{\mathbf{g}} = \left(\mathbf{k}_{\parallel} + \mathbf{g}, \pm\left[q^2 - \left(\mathbf{k}_{\parallel} + \mathbf{g}\right)^2\right]^{1/2}\right) \tag{31}$$

where the $+, -$ sign defines the sign of the z component of the wavevector. We note that when $q^2 < (\mathbf{k}_{\parallel} + \mathbf{g})^2$, the above defines a decaying wave; the positive sign in Eq. (31) describes a wave propagating or decaying to the right, and the negative sign describes a wave propagating or decaying to the left.

We write the electric field of the incident wave in the form

$$\mathbf{E}^{s'}_{in}(\mathbf{r}) = \sum_{i'=1}^{2} [E_{in}]^{s'}_{\mathbf{g}'i'} \exp\left(\mathrm{i}\mathbf{K}^{s'}_{\mathbf{g}'} \cdot \mathbf{r}\right) \hat{\mathbf{e}}_{i'} \tag{32}$$

where $s' = +(-)$ corresponds to a propagating or decaying wave incident on the plane of spheres from the left (right), and $\hat{\mathbf{e}}_1$, $\hat{\mathbf{e}}_2$ are the polar and azimuthal unit vectors, respectively, which are perpendicular to $\mathbf{K}^{s'}_{\mathbf{g}'}$. In the same manner [according to Eq. (31)] we define, for given $\mathbf{k}_{\parallel}$ and q, a wavevector $\mathbf{K}^{s}_{\mathbf{g}}$ and the corresponding $\hat{\mathbf{e}}_i$ for any $\mathbf{g}$ and $s = \pm$. In this way, we can expand the electric-field component of an EM wave into p- and s-polarized transverse plane waves, i.e., polarized along $\hat{\mathbf{e}}_1$ and $\hat{\mathbf{e}}_2$, respectively. We note that, in the case of a decaying wave, the unit vectors $\hat{\mathbf{e}}_1$ and $\hat{\mathbf{e}}_2$ are complex, but they are still orthonormal ($\hat{\mathbf{e}}_i \cdot \hat{\mathbf{e}}_j = \delta_{ij}, i, j = 1, 2$). The coefficients a^0_L in the expansion in Eq. (4) of the plane wave in Eq. (32) can be written in the following form

$$\mathrm{a}^0_L = \sum_{i'=1}^{2} A^0_{L;i'}\left(\mathbf{K}^{s'}_{\mathbf{g}'}\right)[E_{in}]^{s'}_{\mathbf{g}'i'}, \quad \text{for} \quad P = E, H \tag{33}$$

where the coefficients $\mathbf{A}^0_L$ are provided by

$$\begin{aligned}\mathbf{A}^0_{Elm}\left(\hat{\mathbf{K}}^{s'}_{\mathbf{g}'}\right) \;=\; & \frac{4\pi\mathrm{i}^l(-1)^{m+1}}{\sqrt{l(l+1)}}\Bigg\{\mathrm{i}\left[\alpha^m_l e^{\mathrm{i}\phi}Y^{-m-1}_l\left(\hat{\mathbf{K}}^{s'}_{\mathbf{g}'}\right) - \alpha^{-m}_l e^{-\mathrm{i}\phi}Y^{-m+1}_l\left(\hat{\mathbf{K}}^{s'}_{\mathbf{g}'}\right)\right]\hat{\mathbf{e}}_1 \\ & - \Big[\alpha^m_l \cos\theta e^{\mathrm{i}\phi}Y^{-m-1}_l\left(\hat{\mathbf{K}}^{s'}_{\mathbf{g}'}\right) + m\sin\theta Y^{-m}_l\left(\hat{\mathbf{K}}^{s'}_{\mathbf{g}'}\right) \\ & + \alpha^{-m}_l \cos\theta e^{-\mathrm{i}\phi}Y^{-m+1}_l\left(\hat{\mathbf{K}}^{s'}_{\mathbf{g}'}\right)\Big]\hat{\mathbf{e}}_2\Bigg\},\end{aligned} \tag{34}$$

and

$$\mathbf{A}^0_{Hlm}\left(\hat{\mathbf{K}}^{s'}_{\mathbf{g}'}\right) = \frac{4\pi \mathrm{i}^l(-1)^{m+1}}{\sqrt{l(l+1)}}\Big\{\Big[\alpha_l^m \cos\theta e^{\mathrm{i}\phi} Y_l^{-m-1}(\hat{\mathbf{K}}^{s'}_{\mathbf{g}'}) + m\sin\theta Y_l^{-m}\left(\hat{\mathbf{K}}^{s'}_{\mathbf{g}'}\right) + \alpha_l^{-m}\cos\theta e^{-\mathrm{i}\phi} Y_l^{-m+1}\left(\hat{\mathbf{K}}^{s'}_{\mathbf{g}'}\right)\Big]\hat{\mathbf{e}}_1 + \mathrm{i}\Big[\alpha_l^m e^{\mathrm{i}\phi} Y_l^{-m-1}\left(\hat{\mathbf{K}}^{s'}_{\mathbf{g}'}\right) - \alpha_l^{-m} e^{-\mathrm{i}\phi} Y_l^{-m+1}\left(\hat{\mathbf{K}}^{s'}_{\mathbf{g}'}\right)\Big]\hat{\mathbf{e}}_2\Big\}, \tag{35}$$

where θ, ϕ are the angular variables $(\hat{\mathbf{K}}^{s'}_{\mathbf{g}'})$ of $\mathbf{K}^{s'}_{\mathbf{g}'}$.

Because of the 2D periodicity of the plane of (single or clusters of) scatterers, the wave scattered from it, when the wave in Eq. (32) is incident upon it, has the following form

$$\mathbf{E}_{sc}(\mathbf{r}) = \sum_{\mathbf{R}_n} \exp\left(\mathrm{i}\mathbf{k}_\parallel \cdot \mathbf{R}_n\right) \sum_L b_L^+ \mathbf{H}_L(\mathbf{r}_n) \tag{36}$$

where $\mathbf{r}_n = \mathbf{r} - \mathbf{R}_n$. The coefficients b_L^+, which depend linearly on the amplitude of the incident wave, can be written as follows

$$\mathrm{b}_L^+ = \sum_{i'=1}^{2} B^+_{L;i'}\left(\mathbf{K}^{s'}_{\mathbf{g}'}\right)[E_{in}]^{s'}_{\mathbf{g}'i'}. \tag{37}$$

We obtain $\mathbf{B}_L^+$ in terms of the coefficients $\mathbf{A}_L^0$ of Eqs. (34) and (35), by solving the following system of linear equations [5, 6]

$$\sum_{L'}\left[\delta_{LL'} - \sum_{L''} T_{LL''}\Omega_{L''L'}\right] B^+_{L';i'}\left(\mathbf{K}^{s'}_{\mathbf{g}'}\right) = \sum_{L'} T_{LL'}\mathrm{A}^0_{L';i'}\left(\mathbf{K}^{s'}_{\mathbf{g}'}\right). \tag{38}$$

The matrix elements $\Omega_{LL'}$ depend on the geometry of the plane, on the reduced wavevector $\mathbf{k}_\parallel$ and on the frequency ω of the incident wave. They are the Fourier transform of the $\Omega^{nn'}_{LL'}$ introduced in Sec. 5 (explicit relations of which are provided elsewhere [16]). The scattering matrix $T_{LL'}$ for a single sphere is provided by Eqs. (10) and (11). For a single non-spherical scatterer, the T-matrix $T_{LL'}$ is provided numerically by solving Eq. (20). For a cluster of spheres, $T_{LL'}$ is provided by Eq. (29).

Finally, the scattered wave in Eq. (36) is expressed as a sum of plane waves as follows

$$\mathbf{E}^s_{sc}(\mathbf{r}) = \sum_{i=1}^{2}\sum_{\mathbf{g}} [E_{sc}]^s_{\mathbf{g}i} \exp\left(\mathrm{i}\mathbf{K}^s_{\mathbf{g}}\cdot\mathbf{r}\right)\hat{\mathbf{e}}_i \tag{39}$$

where the superscript $s = +(-)$ holds for $z > 0$ ($z < 0$). Though the scattered wave consists, in general, of a number of diffracted beams corresponding to different $\mathbf{g}$ vectors, only beams for which $K^s_{\mathbf{g}z}$ is real constitute propagating waves. The coefficients in Eq. (39) are given by

$$[E_{sc}]^s_{\mathbf{g}i} = \sum_L \Delta_{L;i}\left(\mathbf{K}^s_{\mathbf{g}}\right) B^+_{L;i}\left(\mathbf{K}^{s'}_{\mathbf{g}'}\right) \tag{40}$$

where $\Delta_{L;i}(\mathbf{K}^s_{\mathbf{g}})$ are provided by

$$\boldsymbol{\Delta}_{Elm}\left(\mathbf{K}^s_{\mathbf{g}}\right) = \frac{2\pi(-\mathrm{i})^l}{qA_0K^+_{\mathbf{g}z}\sqrt{l(l+1)}}\Big\{\mathrm{i}\Big[\alpha_l^{-m}e^{\mathrm{i}\phi}Y_l^{m-1}\left(\hat{\mathbf{K}}^s_{\mathbf{g}}\right) - \alpha_l^m e^{-\mathrm{i}\phi}Y_l^{m+1}\left(\hat{\mathbf{K}}^s_{\mathbf{g}}\right)\Big]\hat{\mathbf{e}}_1 - \Big[\alpha_l^{-m}\cos\theta e^{\mathrm{i}\phi}Y_l^{m-1}\left(\hat{\mathbf{K}}^s_{\mathbf{g}}\right) - m\sin\theta Y_l^m\left(\hat{\mathbf{K}}^s_{\mathbf{g}}\right) + \alpha_l^m\cos\theta e^{-\mathrm{i}\phi}Y_l^{m+1}\left(\hat{\mathbf{K}}^s_{\mathbf{g}}\right)\Big]\hat{\mathbf{e}}_2\Big\}, \tag{41}$$

$$\boldsymbol{\Delta}_{Hlm}\left(\mathbf{K}^s_{\mathbf{g}}\right) = \frac{2\pi(-\mathrm{i})^l}{qA_0K^+_{\mathbf{g}z}\sqrt{l(l+1)}}\Big\{\Big[\alpha_l^{-m}\cos\theta e^{\mathrm{i}\phi}Y_l^{m-1}\left(\hat{\mathbf{K}}^s_{\mathbf{g}}\right) - m\sin\theta Y_l^m\left(\hat{\mathbf{K}}^s_{\mathbf{g}}\right) + \alpha_l^m\cos\theta e^{-\mathrm{i}\phi}Y_l^{m+1}\left(\hat{\mathbf{K}}^s_{\mathbf{g}}\right)\Big]\hat{\mathbf{e}}_1 + \mathrm{i}\Big[\alpha_l^{-m}e^{\mathrm{i}\phi}Y_l^{m-1}\left(\hat{\mathbf{K}}^s_{\mathbf{g}}\right) - \alpha_l^m e^{-\mathrm{i}\phi}Y_l^{m+1}\left(\hat{\mathbf{K}}^s_{\mathbf{g}}\right)\Big]\hat{\mathbf{e}}_2\Big\}, \tag{42}$$

where θ, ϕ denote the angular variables ($\hat{\mathbf{K}}^s_{\mathbf{g}}$) of $\mathbf{K}^s_{\mathbf{g}}$. We note that the z component of $\mathbf{K}^s_{\mathbf{g}}$ (denoted by $K^s_{\mathbf{g}z}$) can be real or imaginary. We point out that according to Eq. (40), $[E_{sc}]^s_{\mathbf{g}i}$ depend on the incident plane wave through the coefficients $B^+_{L;i'}(\mathbf{K}^{s'}_{\mathbf{g}'})$. These coefficients are evaluated for an incident plane wave with parallel wavevector $\mathbf{k}_\parallel + \mathbf{g}'$, incident from the left (right) corresponding to $s' = +(-)$, with an electric field, along the i'th direction, of magnitude equal to unity. In other words, $B^+_{L;i'}(\mathbf{K}^{s'}_{\mathbf{g}'})$ are calculated from Eq. (38) by substituting in the right-hand side of this equation $A^0_{L;i'}(\mathbf{K}^{s'}_{\mathbf{g}'})$ from Eqs. (34) and (35).

For example, when a plane wave in Eq. (32) is incident on the plane of scatterers from the left, the transmitted wave (incident + scattered) on the right of the plane of scatterers is given by

$$\mathbf{E}^+_{tr}(\mathbf{r}) = \sum_{i=1}^{2} \sum_{\mathbf{g}} [E_{tr}]^+_{\mathbf{g}i} \exp\left(\mathrm{i}\mathbf{K}^+_{\mathbf{g}} \cdot \mathbf{r}\right) \hat{\mathbf{e}}_i, \quad z > 0 \tag{43}$$

with

$$[E_{tr}]^+_{\mathbf{g}i} = [E_{in}]^+_{\mathbf{g}'i}\, \delta_{\mathbf{g}\mathbf{g}'} + [E_{sc}]^+_{\mathbf{g}i} = \sum_{i'} M^{++}_{\mathbf{g}i;\mathbf{g}'i'}\, [E_{in}]^+_{\mathbf{g}'i'} \tag{44}$$

and the reflected wave by

$$\mathbf{E}^-_{rf}(\mathbf{r}) = \sum_{i=1}^{2} \sum_{\mathbf{g}} [E_{rf}]^-_{\mathbf{g}i} \exp\left(\mathrm{i}\mathbf{K}^-_{\mathbf{g}} \cdot \mathbf{r}\right) \hat{\mathbf{e}}_i, \quad z < 0 \tag{45}$$

with

$$[E_{rf}]^-_{\mathbf{g}i} = [E_{sc}]^-_{\mathbf{g}i} = \sum_{i'} M^{-+}_{\mathbf{g}i;\,\mathbf{g}'i'}\, [E_{in}]^+_{\mathbf{g}'i'} \tag{46}$$

Similarly, we can define the transmission matrix elements $M^{--}_{\mathbf{g}i;\,\mathbf{g}'i'}$ and the reflection matrix elements $M^{+-}_{\mathbf{g}i;\mathbf{g}'i'}$ for a plane wave incident on the plane of scatterers from the right. Using Eq. (40) we obtain

$$M^{\mathrm{ss}'}_{\mathbf{g}i;\,\mathbf{g}'i'} = \delta_{ss'}\delta_{\mathbf{g}\mathbf{g}'}\delta_{ii'} + \sum_{L} \Delta_{L;i}\left(\mathbf{K}^s_{\mathbf{g}}\right) B^+_{L;i'}\left(\mathbf{K}^{s'}_{\mathbf{g}'}\right) \tag{47}$$

The matrix elements $M^{ss'}_{\mathbf{g}i;\,\mathbf{g}'i'}$ obey the following symmetry relation [5, 6]

$$M^{-\mathrm{s}-\mathrm{s}'}_{\mathbf{g}i;\,\mathbf{g}'i'} = (-1)^{i+i'} M^{\mathrm{ss}'}_{\mathbf{g}i;\,\mathbf{g}'i'} \tag{48}$$

The transmission/reflection matrices of a stack of planes of scatterers with the same 2D periodicity parallel to the xy plane are obtained from the transmission/reflection matrices of the individual planes [5, 6]. We express the waves on the left of a given plane of scatterers with respect to an origin, $\mathbf{A}_l$, on the left of the plane at $-\mathbf{d}_l$ from its centre and the waves on the right of this plane with respect to an origin, $\mathbf{A}_r$, on the right of the plane at $\mathbf{d}_r$ from its centre. With the above choice of origins the transmission/reflection matrix elements of a plane of (single or clusters of) scatterers become

$$\begin{aligned}
Q^{\mathrm{I}}_{\mathbf{g}i;\,\mathbf{g}'i'} &= M^{++}_{\mathbf{g}i;\,\mathbf{g}'i'} \exp\Big(\mathrm{i}(\mathbf{K}^+_{\mathbf{g}} \cdot \mathbf{d}_r + \mathbf{K}^+_{\mathbf{g}'} \cdot \mathbf{d}_l)\Big) \\
Q^{\mathrm{II}}_{\mathbf{g}i;\,\mathbf{g}'i'} &= M^{+-}_{\mathbf{g}i;\,\mathbf{g}'i'} \exp\Big(\mathrm{i}(\mathbf{K}^+_{\mathbf{g}} \cdot \mathbf{d}_r - \mathbf{K}^-_{\mathbf{g}'} \cdot \mathbf{d}_r)\Big) \\
Q^{\mathrm{III}}_{\mathbf{g}i;\,\mathbf{g}'i'} &= M^{-+}_{\mathbf{g}i;\,\mathbf{g}'i'} \exp\Big(-\mathrm{i}(\mathbf{K}^-_{\mathbf{g}} \cdot \mathbf{d}_l - \mathbf{K}^+_{\mathbf{g}'} \cdot \mathbf{d}_l)\Big) \\
Q^{\mathrm{IV}}_{\mathbf{g}i;\,\mathbf{g}'i'} &= M^{--}_{\mathbf{g}i;\,\mathbf{g}'i'} \exp\Big(-\mathrm{i}(\mathbf{K}^-_{\mathbf{g}} \cdot \mathbf{d}_l + \mathbf{K}^-_{\mathbf{g}'} \cdot \mathbf{d}_r)\Big)
\end{aligned} \tag{49}$$

In what follows we shall write the above matrix elements in compact form: $\mathbf{Q}^{\mathrm{I}}$, $\mathbf{Q}^{\mathrm{II}}$, $\mathbf{Q}^{\mathrm{III}}$, and $\mathbf{Q}^{\mathrm{IV}}$ which implies a definite sequence in the ordering of the indices: $\mathbf{g}_1 1$, $\mathbf{g}_1 2$, $\mathbf{g}_2 1$, $\mathbf{g}_2 2$, ...

5.3. Multiple-Scattering within a Slab of Many 2D Planes of Scatterers

We obtain the transmission and reflection matrices of two successive 2D planes of scatterers, 1 and 2, by combining the matrices of the two elements, as shown schematically in Fig. 1. It is worth noting that each element need not be exclusively a single plane of scatterers, but it may comprise many 2D planes of identical or different scatterers wherein each scatterer may be a single non-spherical objects or a cluster of non-spherical objects. One can easily prove that the transmission and reflection matrices for the pair of elements, denoted by $\mathbf{Q}(1,2)$, are

$$\begin{aligned}
\mathbf{Q}^{\mathrm{I}}(1,2) &= \mathbf{Q}^{\mathrm{I}}(2)\left[\mathbf{I}-\mathbf{Q}^{\mathrm{II}}(1)\mathbf{Q}^{\mathrm{III}}(2)\right]^{-1}\mathbf{Q}^{\mathrm{I}}(1)\\
\mathbf{Q}^{\mathrm{II}}(1,2) &= \mathbf{Q}^{\mathrm{II}}(2)+\mathbf{Q}^{\mathrm{I}}(2)\mathbf{Q}^{\mathrm{II}}(1)\times\left[\mathbf{I}-\mathbf{Q}^{\mathrm{III}}(2)\mathbf{Q}^{\mathrm{II}}(1)\right]^{-1}\mathbf{Q}^{\mathrm{IV}}(2)\\
\mathbf{Q}^{\mathrm{III}}(1,2) &= \mathbf{Q}^{\mathrm{III}}(1)+\mathbf{Q}^{\mathrm{IV}}(1)\mathbf{Q}^{\mathrm{III}}(2)\times\left[\mathbf{I}-\mathbf{Q}^{\mathrm{II}}(1)\mathbf{Q}^{\mathrm{III}}(2)\right]^{-1}\mathbf{Q}^{\mathrm{I}}(1)\\
\mathbf{Q}^{\mathrm{IV}}(1,2) &= \mathbf{Q}^{\mathrm{IV}}(1)\left[\mathbf{I}-\mathbf{Q}^{\mathrm{III}}(2)\mathbf{Q}^{\mathrm{II}}(1)\right]^{-1}\mathbf{Q}^{\mathrm{IV}}(2)
\end{aligned} \tag{50}$$

All matrices refer of course to the same ω and $\mathbf{k}_{\|}$. We note in particular that the waves on the left (right) of the pair of elements are referred to an origin at $-\mathbf{d}_l(1)$ $(+\mathbf{d}_r(2))$ from the centre of the 1st (2nd) element.

It is obvious that we can repeat the process to obtain the transmission and reflection matrices of three elements, by combining those of the pair of elements with those of the third element, and that we can in a similar fashion repeat the process to obtain the scattering matrices of a slab consisting of any finite number of elements. However, a slab may consist of a number of identical elements stacked together along the z-axis (normal to the surface of the slab). We assume that the slab consists of 2^N elements, where $N = 0, 1, 2, \ldots$.

Having calculated the $\mathbf{Q}$-matrix elements of a single element, we obtain those of the slab, by a doubling-layer scheme as follows: we first obtain the $\mathbf{Q}$-matrix of two consecutive elements in the manner described above; then, using as units the $\mathbf{Q}$-matrix of a pair of elements, we obtain those of four consecutive elements, and in this way, by doubling the number of elements at each stage we finally obtain the $\mathbf{Q}$-matrix elements of the 2^N elements of the slab.

In summary, for a plane wave $\sum_i [E_{in}]^+_{\mathbf{g}'i}\exp(\mathrm{i}\mathbf{K}^+_{\mathbf{g}'}\cdot(\mathbf{r}-\mathbf{A}_L))\hat{e}_i$, incident on the slab from the left, we finally obtain a reflected wave $\sum_{\mathbf{g}i}[E_{rf}]^-_{\mathbf{g}i}\exp(\mathrm{i}\mathbf{K}^-_{\mathbf{g}}\cdot(\mathbf{r}-\mathbf{A}_L))\hat{e}_i$ on the left of the slab and a transmitted wave $\sum_{\mathbf{g}i}[E_{tr}]^+_{\mathbf{g}i}\exp(\mathrm{i}\mathbf{K}^+_{\mathbf{g}}\cdot(\mathbf{r}-\mathbf{A}_R))\hat{e}_i$ on the right of the slab, where $\mathbf{A}_L$ $(\mathbf{A}_R)$ is the appropriate origin

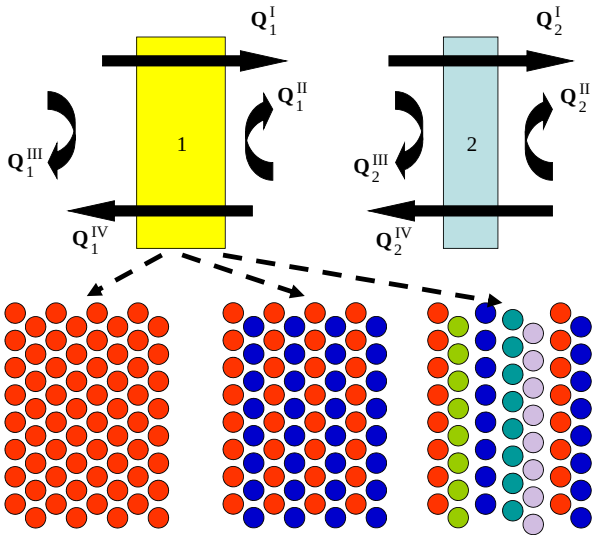

Figure 1. Schematic definition of the scattering $\mathbf{Q}$-matrices of two finite slabs. For the calculation of the scattering matrix of the pair of slabs one takes into account all the multiple-scattering paths between the two constituent slabs.

on the left (right) of the slab. We have

$$[E_{tr}]^{+}_{\mathbf{g}i} = \sum_{i'} Q^{\mathrm{I}}_{\mathbf{g}i;\,\mathbf{g}'i'}\,[E_{in}]^{+}_{\mathbf{g}'i'} \tag{51}$$

$$[E_{rf}]^{-}_{\mathbf{g}i} = \sum_{i'} Q^{\mathrm{III}}_{\mathbf{g}i;\,\mathbf{g}'i'}\,[E_{in}]^{+}_{\mathbf{g}'i'} \tag{52}$$

where the $\mathbf{Q}$-matrix elements are those of the whole slab.

When we have calculated the transmitted wave in Eq. (51) and reflected wave in Eq. (52), corresponding to the given incident wave, we can obtain the transmittance $\mathcal{T}$ and reflectivity $\mathcal{R}$ of the slab. $\mathcal{T}(\mathcal{R})$ is defined as the ratio of the flux of the transmitted (reflected) wave to the flux of the incident wave. Integrating the Poynting vector over the xy-plane, on the appropriate side of the slab and taking the time average over a period $T = 2\pi/\omega$, we obtain

$$\begin{aligned}
\mathcal{T} &= \frac{\sum_{\mathbf{g},i}[E_{tr}]^{+}_{\mathbf{g}i}\left([E_{tr}]^{+}_{\mathbf{g}i}\right)^{*}K^{+}_{\mathbf{g}z}}{\sum_{i}[E_{in}]^{+}_{\mathbf{g}'i}\left([E_{in}]^{+}_{\mathbf{g}'i}\right)^{*}K^{+}_{\mathbf{g}'z}} \\
\mathcal{R} &= \frac{\sum_{\mathbf{g},i}[E_{rf}]^{-}_{\mathbf{g}i}\left([E_{rf}]^{-}_{\mathbf{g}i}\right)^{*}K^{+}_{\mathbf{g}z}}{\sum_{i}[E_{in}]^{+}_{\mathbf{g}'i}\left([E_{in}]^{+}_{\mathbf{g}'i}\right)^{*}K^{+}_{\mathbf{g}'z}}
\end{aligned} \tag{53}$$

where the $*$ sign denotes complex conjugation as usual. If the structure contains light-absorbing materials, the requirement of energy conservation implies that the absorbance $\mathcal{A}$ of the slab is

$$\mathcal{A} = 1 - \mathcal{T} - \mathcal{R} \tag{54}$$

6. TEST EXAMPLE

The technique presented so far has a hierarchical structure which is demonstrated with the following test cases. Namely, we start by calculating the scattering from a single metallic (gold) nanocube (see Fig. 2), then we proceed to solving the scattering problem for a cluster of gold nanocubes (see Fig. 3) whereby we solve the problem of light scattering of a square lattice of clusters of nanocubes (see Fig. 4) or from a slab of square lattices (layers) of clusters of nanocubes (see Fig. 5).

First we find the scattering T-matrix as well as the corresponding extinction, absorption and scattering spectra for 100 nm gold nanocube based on the point-matching method of Sec. 4.2. The dielectric function of gold is taken from experiment [29]. Fig. 2 shows the cross-sections for linearly polarized light incident normally on a nanocube face. The curves are obtained by discretizing the cubes into $10^3 = 1000$ dipoles while the cutoff in the angular-momentum expansion is taken $l_{\max} = 7$. We note that the cross sections already converge for a lower cutoff ($l_{\max} = 4$); however, for the periodic photonic structures of gold nanocubes studied right below, a higher angular-momentum cutoff ($l_{\max} = 7$) is needed to achieve convergence [4–6]. The evident peak in all three curves of Fig. 2 is attributed to the excitation of the surface plasmon resonance at 540 nm (when defined from the absorption cross section).

A note on the numerical accuracy of the presented method. The multiple-scattering methods are, in general, semi-analytical methods and therefore contain minimum numerical errors. The only numerically involved part of the presented hierarchical multiple-scattering theory is the point-matching method which provides the scattering T-matrix of a general non-spherical object. The relative error in the point-matching method is 1.3% [17] which is also the principle numerical error of the entire method.

Having calculated the T-matrix for a single 100 nm gold nanocube as described in Sec. 4.2, we apply the real-space multiple-scattering formalism of Sec. 5 to obtain the total scattering matrix, i.e., Eq. (29) of the cluster of nanocubes shown in Fig. 3. The corresponding extinction, scattering and absorption spectra can be found from Eq. (15) of [7] which is based on the elements of a given T-matrix. The general features of all spectra are similar to those of a single nanocube (Fig. 2) except from a 'fat tail' in the extinction and scattering spectra at long wavelengths which is absent for a single nanocube. This is an expected result stemming from the interaction of the surface-plasmons among the nanocubes of the cluster.

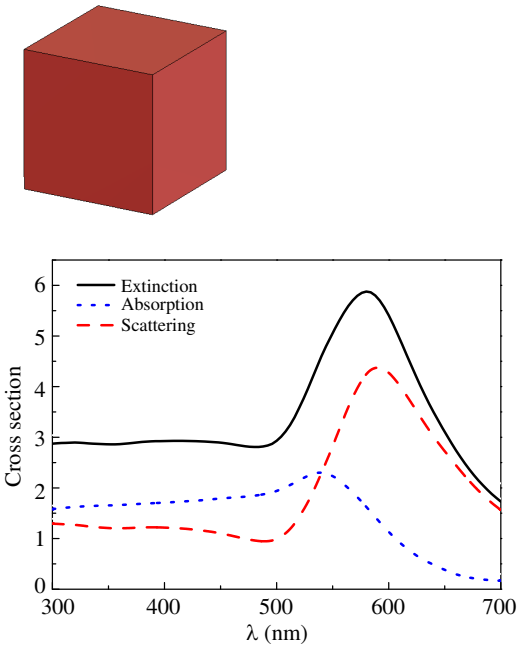

Figure 2. (Color online) Extinction (solid), scattering (dashed) and absorption (dotted line) cross sections (in arbitrary units) for light incident normally on one of the faces of gold nanocube (shown in the top) with 100 nm edge. The curves are calculated by assuming 1000 dipoles in the DDA and $l_{\max} = 7$ in the angular momentum expansion.

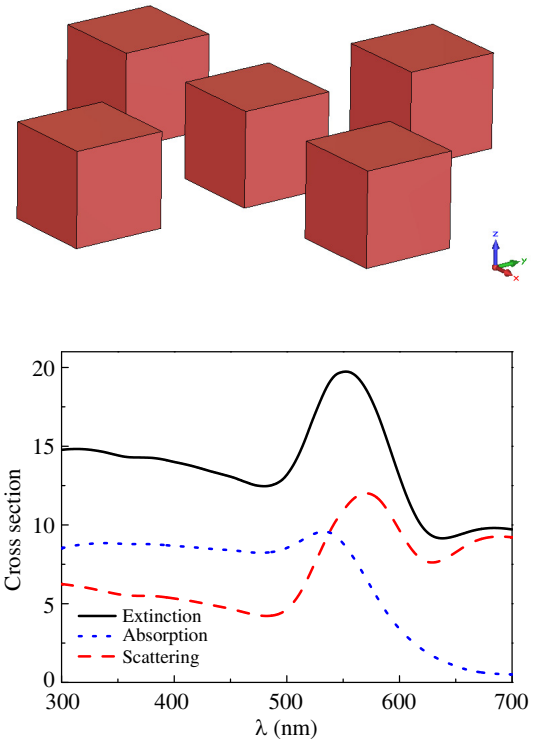

Figure 3. (Color online) Extinction (solid), scattering (dashed) and absorption (dotted line) cross sections (in arbitrary units) for light incident normally on the cluster of 100 nm gold nanocubes (shown in the top). The cubes are positioned at the points: $(0,0,0), (200,0,0), (-200,0,0), (0,200,0), (0,-200,0)$ in nm units. The curves are calculated by assuming $l_{\max} = 7$ in the angular momentum expansion.

The total T-matrix [Eq. (29)] for the cluster of nanocubes is embedded within the LMS formalism [see Eq. (38)] whereby we can model the EM response of 2D or 3D lattices which possess the cluster of nanocubes as unit cell shown in Fig. 3. Indeed, in Fig. 4 we show the transmittance, reflectance and absorbance spectra for light incident normally on a 2D square lattice of clusters of nanocubes of Fig. 3. In the absorbance spectrum, apart from the main peak around 545 nm due to the surface-plasmon excitation of the nanocubes, there is a distinct peak at $\lambda = \alpha/2 = 325$ nm (corresponding to a dip in the transmittance spectrum) as well as a dip at $\lambda = \alpha/\sqrt{2} = 459$ nm (corresponding to a peak of the transmittance spectrum). Both the above features stem from the periodicity of the nanocube array and are characterized as Wood anomalies; they correspond to the wavelengths for which the z-component of the wavevector diffracted beams, i.e., the z-component of the wavevector of Eq. (31), is equal to zero. There occurs a Wood anomaly at $\lambda = \alpha = 650$ nm as well, but it is less evident than the other two at $\lambda = 459, 325$ nm.

In Fig. 5, we study a 3D simple cubic crystal whose sites are occupied by the cluster of nanocubes of Fig. 3. Fig. 5(a) shows the frequency band structure (dispersion relation) of a (infinitely periodic) simple cubic crystal of lattice constant of 650 nm. Figs. 5(b) and (c) depict the reflectance and absorbance of light incident normally on finite slabs of the simple cubic crystal of Fig. 5(a). The various slabs consist of 1, 2 and 4 layers (each layer is a 2D square lattice of clusters of nanocubes). Evidently, as the number of layers (slab thickness) increases the absorbance curve increases too, except for longer wavelengths

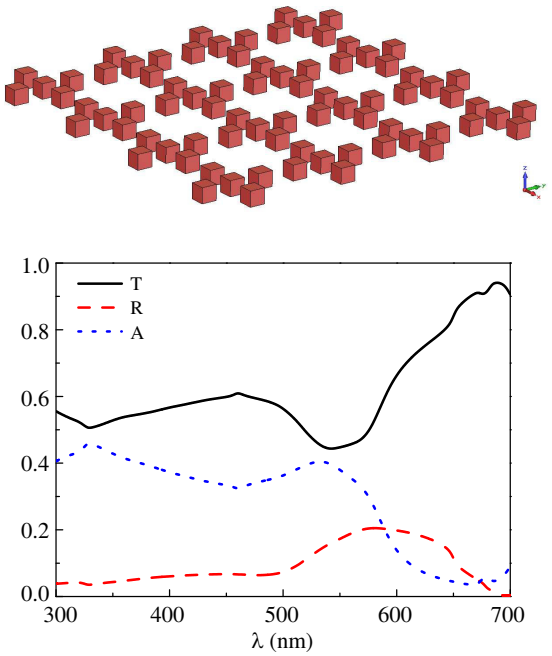

Figure 4. (Color online) Transmittance, reflectance and absorbance for light incident normally on an infinitely periodic 2D square lattice where the unit cell is the cluster of cubes of Fig. 3. The lattice constant $a = 650\,\text{nm}$.

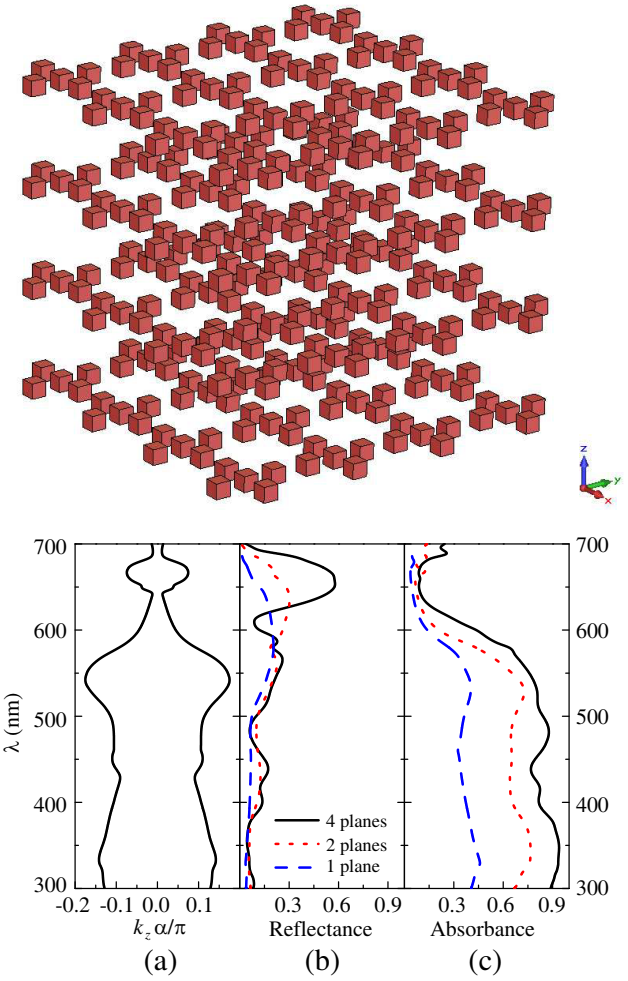

Figure 5. (Color online) (a) Dispersion curves along the $[0, 0, 1]$ crystallographic direction of simple cubic crystal where the periodic unit is the cluster of cubes of Fig. 3. The lattice constant of the simple cubic lattice is $a = 650\,\text{nm}$. (b) Reflectance and (c) absorbance of light incident normally on finite slabs of various thicknesses (number of layers) of the simple cubic crystal of (a).

(above 600 nm) where absorbance is suppressed due to the enhance reflectivity which is because of weak coupling of incident light with the crystal modes within the slab.

7. CONCLUSION

We have presented an extension of the layer-multiple-scattering technique so that it can accommodate clusters of general-shaped scatterers. The developed technique breaks down to two stages of EM multiple-scattering, i.e., within the (finite) cluster of scatterers and within the (infinite) 2D or 3D lattice of clusters. The scattering off a single scatterer is solved via a hybrid discrete-dipole approximation/T-matrix method based on a point-matching module. The developed formalism is applied to the modelling of 2D and 3D periodic lattices consisting of gold nanocubes in terms of the optical properties. The generalization of the layer-multiple-scattering method to many non-spherical scatterers is potentially

useful for thin plasmonic metasurfaces [30] where the corresponding unit cell consists of dissimilar scatterers.

REFERENCES

1. Gonis, A. and W. H. Butler, *Multiple Scattering in Solids*, Springer, New York, 2000.
2. Wang, X., X.-G. Zhang, Q. Yu, and B. N. Harmon, "Multiple-scattering theory for electromagnetic waves," *Phys. Rev. B*, Vol. 47, No. 8, 4161–4167, 1993.
3. Moroz, A., "Density-of-states calculations and multiple-scattering theory for photons," *Phys. Rev. B*, Vol. 51, No. 4, 2068–2081, 1995.
4. Stefanou, N., V. Karathanos, and A. Modinos, "Scattering of electromagnetic waves by periodic structures," *J. Phys.: Condens. Matter*, Vol. 4, No. 36, 7389–7400, 1992.
5. Stefanou, N., V. Yannopapas, and A. Modinos, "Heterostructures of photonic crystals: Frequency bands and transmission coefficients," *Comput. Phys. Commun.*, Vol. 113, No. 1, 49–77, 1998.
6. Stefanou, N., V. Yannopapas, and A. Modinos, "MULTEM 2: A new version of the program for transmission and band-structure calculations of photonic crystals," *Comput. Phys. Commun.*, Vol. 132, No. 1–2, 189–196, 2000.
7. Gantzounis, G. and N. Stefanou, "Layer-multiple-scattering method for photonic crystals of nonspherical particles," *Phys. Rev. B*, Vol. 73, No. 035115, 2006.
8. Gantzounis, G., N. Stefanou, and N. Papanikolaou, "Multiple-scattering calculations for layered phononic structures of nonspherical particles," *Phys. Rev. B*, Vol. 77, No. 214301, 2008.
9. Tserkezis, C., N. Papanikolaou, G. Gantzounis, and N. Stefanou, "Understanding artificial optical magnetism of periodic metal-dielectric-metal layered structures," *Phys. Rev. B*, Vol. 78, No. 165114, 2008.
10. Christofi, A., N. Stefanou, G. Gantzounis, and N. Papanikolaou, "Spiral-staircase photonic structures of metallic nanorods," *Phys. Rev. B*, Vol. 84, No. 125109, 2011.
11. Christofi, A. and N. Stefanou, "Nonreciprocal optical response of helical periodic structures of plasma spheres in a static magnetic field," *Phys. Rev. B*, Vol. 87, No. 115125, 2013.
12. Christofi, A. and N. Stefanou, "Nonreciprocal photonic surface states in periodic structures of magnetized plasma nanospheres," *Phys. Rev. B*, Vol. 88, No. 125133, 2013.
13. Christofi, A. and N. Stefanou, "Layer multiple scattering calculations for nonreciprocal photonic structures," *Int. J. Mod. Phys. B*, Vol. 28, No. 1441012, 2014.
14. Mühlig, S., C. Rockstuhl, V. Yannopapas, T. Bürgi, N. Shalkevich, and F. Lederer, "Optical properties of a fabricated self-assembled bottom-up bulk metamaterial," *Opt. Express*, Vol. 19, No. 10, 9607–9616, 2011.
15. Yannopapas, V. and A. Vanakaras, "Dirac point in the photon dispersion relation of a negative/zero/positive-index plasmonic metamaterial," *Phys. Rev. B*, Vol. 84, No. 045128, 2011.
16. Yannopapas, V. and A. Vanakaras, "Layer-multiple-scattering theory for metamaterials made from clusters of nanoparticles," *Phys. Rev. B*, Vol. 84, No. 085119, 2011.
17. Yannopapas, V., "Layer-multiple-scattering method for photonic structures of general scatterers based on a discrete-dipole approximation/T-matrix point-matching method," *J. Opt. Soc. Am. B*, Vol. 31, No. 3, 631–636, 2014.
18. Jackson, J. D., *Classical Electrodynamics*, Wiley, New York, 1975.
19. Bohren, C. F. and D. R. Huffman, *Absorption and Scattering of Light by Small Particles*, Wiley, New York, 1983.
20. Sainidou, R., N. Stefanou, and A. Modinos, "Green's function formalism for phononic crystals," *Phys. Rev. B*, Vol. 69, No. 064301, 2004.
21. Purcell, E. M. and C. R. Pennypacker, "Scattering and absorption of light by nonspherical dielectric grains," *Astrophys. J.*, Vol. 186, 705–714, 1973.
22. Draine, B. T. and P. J. Flatau, "Discrete-dipole approximation for scattering calculations," *J. Opt. Soc. Am. A*, Vol. 11, No. 4, 1491–1499, 1994.

23. Yurkin, M. A. and A. G. Hoekstra, "The discrete dipole approximation: An overview and recent developments," *J. Quant. Spec. Rad. Transfer*, Vol. 106, No. 1–3, 558–589, 2007.
24. Chaumet, P. C. and A. Rahmani, "Efficient iterative solution of the discrete dipole approximation for magnetodielectric scatterers," *Opt. Lett.*, Vol. 34, No. 7, 917–919, 2009.
25. Loke, V. L. Y., T. A. Nieminen, N. R. Heckenberg, and H. Rubinsztein-Dunlop, "T-matrix calculation via discrete dipole approximation, point matching and exploiting symmetry," *J. Quantit. Spectrosc. Radiat. Transfer*, Vol. 110, No. 14–16, 1460–1471, 2009.
26. Loke, V. L. Y., T. A. Nieminen, S. J. Parkin, N. R. Heckenberg, and H. Rubinsztein-Dunlop, "FDFD/T-matrix hybrid method," *J. Quantit. Spectrosc. Radiat. Transfer*, Vol. 106, No. 1–3, 274–284, 2007.
27. Menzel, C., S. Mühlig, C. Rockstuhl, and F. Lederer, "Multipole analysis of meta-atoms," *Metamaterials*, Vol. 5, No. 2–3, 64–73, 2011.
28. Yannopapas, V. and N. V. Vitanov, "Electromagnetic Greens tensor and local density of states calculations for collections of spherical scatterers," *Phys. Rev. B*, Vol. 75, No. 115124, 2007.
29. Johnson, R. B. and R. W. Christy, "Optical constants of the noble metals," *Phys. Rev. B*, Vol. 6, No. 12, 4370–4379, 1972.
30. Yu, N. and F. Capasso, "Flat optics with designer metasurfaces," *Nat. Mater.*, Vol. 13, 139–150, 2014.